13
Microcasting

G. Baumeister, J. Haußelt, S. Rath, R. Ruprecht, Institute for Materials Research III (IMF III), Forschungszentrum Karlsruhe, Germany

Abstract

Microcasting is a metal forming process based on the well-known lost-wax – lost-mold technology of investment casting. The further development of this technique for casting structures in the range of some tens of micrometers requires special patterns, investments and casting parameters. First, this chapter describes the general casting process, highlighting differences from conventional dental and jewelry casting. Additionally, the parameters of a typical microcasting process are given. Next, some alloys used for microcasting and their chemical compositions, melting and casting temperatures and phase transitions during the solidification process are described in detail. Thereafter, the two basic investments used for microcasting and the influence of the investment on the surface roughness of the cast parts are discussed. Finally, cast microparts are shown and their properties such as microstructure, dimensional accuracy, surface roughness, mechanical properties, smallest achievable structure size and highest obtainable flow length and aspect ratio are presented.

Keywords

investment casting; dental casting; gold base alloy; bronze; CoCrMo alloy

Advanced Micro and Nanosystems Vol. 4. Microengineering of Metals and Ceramics.
Edited by H. Baltes, O. Brand, G. K. Fedder, C. Hierold, J. Korvink, O. Tabata

ISBN: 3-527-31493-8

13.1 Introduction

Microcasting is the manufacturing process of small structures in the micrometer range or of larger parts carrying microstructures by using a metal melt which is cast into a microstructured mold. Fields of application are, e.g., instruments for minimal invasive surgery, dental devices and instruments for biotechnology. Additionally, the manufacturing of miniaturized devices for mechanical engineering is a desired outcome.

At present, two different techniques for casting structures in the micrometer range are known: capillary action microcasting and microcasting based on investment casting. The first manufacturing method was developed by Bach et al. [1] and Moehwald et al. [2]. They applied capillary action microcasting for form filling of structures in the range of some micrometers. Similar to die casting, this technique uses a permanent mold which can be opened in order to remove the cast structure. The cavities in the mold are shaped by high-precision grinding [2]. For casting, two different principles to fill these cavities exist: the suction principle and the displacement principle [1]. In the first case the melt is sucked into a specially coated mold by the capillary pressure. In the second case the casting alloy is melted inside the divisible mold and fills the microstruc-

tured cavities owing to the capillary force. Subsequently pressure is applied to the mold to displace the excess melt through the slit. Owing to absorption of the coating during solidification, the casting detaches from the mold's surface, but at the same time the alloy composition changes slightly compared with the original material. In capillary action microcasting the castable geometries are limited to structures which can be filled by application of capillary forces. Microcasting based on the investment casting technique, which will be discussed in the following, does not suffer from these limitations.

13.2 Investment Casting

Microcasting, also named microprecision casting [3, 4], is generally identified with the investment casting process, a casting technology also known as the lost-wax, lost-mold technique [5, 6]. This forming process excels in near net shape manufacturing and is an established technology with great freedom in design [7]. It offers the chance to produce very complicated formed parts in metal even with undercuts. Another advantage of the investment casting process over other shaping processes is the rapidity of the casting procedure itself and the low loss of material due to the possibility of recycling the runners and sprues. However, the process cannot be fully automated, so it is best suited for small and medium series and for parts with highly complex shape. This is the reason why investment casting has, in addition to technical application, a high relevance for jewelry and dental casting. For both applications, precise manufacturing is achieved [8–13], especially by using precious alloys. For jewelry and dental casting, the sizes of the produced parts are in the millimeter up to the centimeter range with structural details in the millimeter and submillimeter ranges [1]. Further development and improvement of these techniques allowed the casting of microparts with structural details even in the micrometer range, which was confirmed by the replication of small-scale LIGA structures (see Section 13.2.1.1) with high accuracy [15]. The new microtechnology, derived from the conventional production process, requires different pattern materials, other investments, special alloys and other casting parameters compared with the standard investment casting process. Additionally, microcast parts cannot be machined mechanically after manufacturing. Sand blasting, as applied in dental and jewelry casting, cannot be used to remove residue of the investment, nor can surfaces be polished to increase their quality. Sand blasting would reduce the sharpness of the edges and therefore influence the accuracy of the part, and polishing is not possible because of their small size. Therefore, precious alloys are particularly suitable for microcasting, because here the investment can be removed chemically from the cast metal part using hydrofluoric acid without influencing the cast part. Recent progress in the development of investments, however, opened the possibility of casting microstructures with bronze as a non-precious alloy [17]. In the following, the typical microcasting process will

be illustrated first. Later, details on the alloys and investments and variables specifically influencing this process are given.

13.2.1 General Process

The microcasting process, which is described in Section 13.2.1.1, has enormous potential in manufacturing microparts of high quality without the need for further processing, as opposed to the dental and jewelry casting technique. The patterns used in the microcasting process (see Section 13.2.1.2) guarantee a higher strength and are thus of advantage when assembling microstructures. Sections 13.2.1.3–13.2.1.5 give the basics on melting, casting and solidification.

13.2.1.1 Process Description

The microcasting process itself is based on the lost-wax, lost-mold technique. It is widely comparable to casting of dental protheses or jewelry [18]. In contrast to the wax patterns used there, microtechnology mostly works with injection-molded plastic patterns which have much higher mechanical strength. The improved mechanical properties permit easier handling and assembling of the pattern during the manufacturing process.

The shaping of the microcavities in the mold insert, used for injection molding, can be achieved by several methods. We applied mainly the technique of micromilling [19–21], which is a further development and improvement of the standard milling process towards miniaturized manufacturing (see Chapter 4), but in some cases also microelectro discharge machining [22, 23]. More details on the latter process can be found in Chapter 7. Other ways for the production of microstructured mold inserts are the laser technique [24–26] and the LIGA process [28–30]. The LIGA process, which is described in detail in Chapter 8, includes a lithographic and a galvanic process and is beneficial for microreplication owing to the very good surface quality of the mold inserts and the high potential of generating minimum structures. However, in contrast to the milling process, which allows the production of free form faces and real 3D structures, the LIGA technique is limited to 2.5-dimensional structures because of their necessarily vertical walls.

The microcasting process requires a lost plastic pattern to be mounted on a gate and feeding system made of wax (Fig. 13-1). The assembly is then completely embedded in a ceramic slurry. This process differs from the technical investment casting process where normally a ceramic shell is built-up by repeatedly dipping the pattern in a ceramic slurry followed by stuccoing. After drying, the ceramic is sintered, resulting in a ceramic mold with high mechanical strength. Simultaneously, the plastic melts during the burning process and is pyrolyzed.

In order to fill the mold with the metallic melt, either the vacuum pressure casting or the centrifugal casting technique can be used. In the first case, the

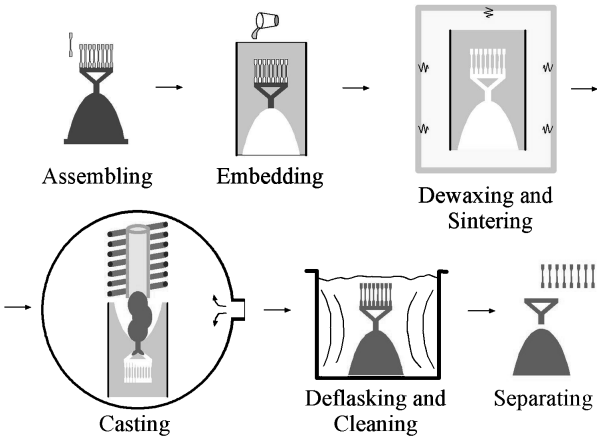

Fig. 13-1 Scheme of investment casting process

ceramic investment mold is evacuated, then the melt is poured into the mold, filling the cavity only due to gravitational forces. After that, pressure is applied to the melt. In the second case, the centrifugal force is used for form filling. Both techniques will be explained later in detail. After solidification, the investment is mechanically removed without destroying or influencing the cast surface. Depending on the casting alloy and the investment material, additional chemical cleaning processes may be sometimes necessary. Finally, the single parts are separated from the runner system. Unlike dental or jewelry casting, there is no further treatment such as grinding or polishing of the cast surface. This is due to the much smaller geometry and inapproachability of details on cast microparts and also to the necessity for high contour precision without any rounding of the edges.

Fig. 13-2 shows the most important replication steps for the example of a microturbine plate. On the left, the mold insert for injection molding of the pattern, the negative form, is shown. It is made by micromilling in brass. In the

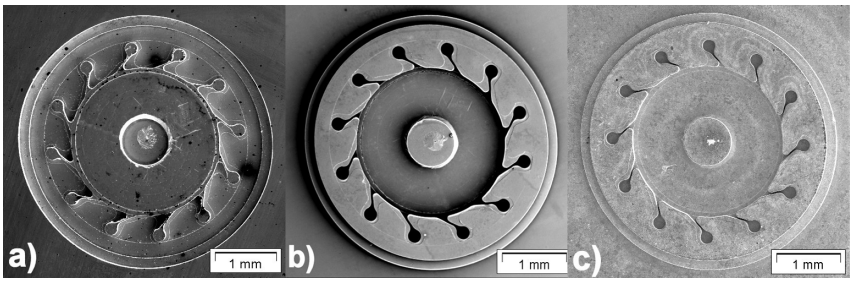

Fig. 13-2 a) Mold insert for injection molding, b) PMMA pattern, c) cast part made in gold base alloy Stabilor® G

center is the injection-molded plastic turbine plate made of PMMA [poly(methyl methacrylate)]. This is the positive pattern required for microcasting. The plastic pattern is replicated by the investment and forms the negative mold. The third replication process – the real casting – yields the desired positive form, in this case made of a gold base alloy (right). It is worth mentioning that the replication is so precise that even scratches with depths of a few micrometers in the mold insert for injection molding are perfectly replicated on the cast part.

The investment casting procedure for manufacturing microparts is influenced by many different parameters. The most important ones are the casting alloy, the ceramic investment, the preheating temperature of the mold and the casting pressure. The molten casting alloys must exhibit a low viscosity in order to fill the small microstructures completely. Additionally, a minor tendency for oxidation is of high interest. For the ceramic investment, the most important factors are the ability for high-precision replication, an expansion behavior adjusted to the alloy used and a low surface roughness. The preheating temperature and the pressure influence the entire form filling process [31] and, as a consequence, the achievable grain size and the resulting mechanical properties.

13.2.1.2 **Pattern Design**

For cost-effective casting, the assembly of single patterns in form of a so-called tree is necessary, whereas the design rules of good castability should be considered to allow homogeneous form filling of all mounted structures. In microcasting, single polymer patterns are normally fixed with wax. As an example, Fig. 13-3a shows a pattern with 15 injection-molded polymer tensile test specimens fixed on a sprue system made of wax. In Fig. 13-3b, the resulting cast part (gold base alloy) can be seen. Single microstructured patterns should be made at least with a small runner owing to the difficult handling of the small parts. Forming of complete plastic or wax assemblies is even better. Especially patterns which are injection-molded on a substrate plate proved to be advantageous because the substrate plate can be used as feeder. However, the melt flow

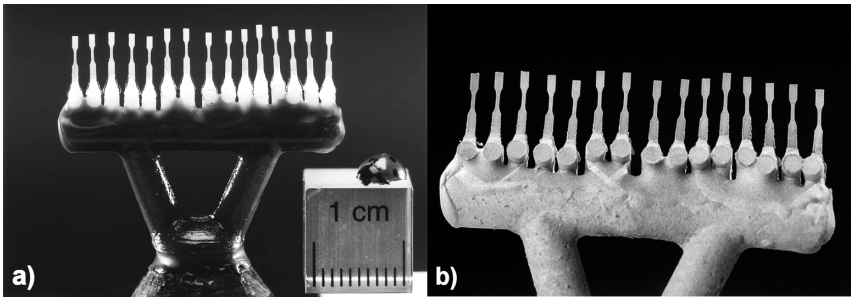

Fig. 13-3 a) Pattern with 15 injection-molded polymer tensile test specimens fixed on a sprue system made of wax; b) equivalent cast part manufactured in a gold base alloy

in the plate is not easy to control. In industry, similar problems are solved by simulating the casting process. For microdimensions such specialized tools are not yet available.

Like patterns for macrocasting, patterns for microcasting should be constructed according to the well-known design rules for casting [32–35]. In order to produce faultless patterns, different wall thicknesses and sharp edges should be avoided [36]. Furthermore, the form filling process is of great importance. The cross-sectional thickness of the sprue system should increase in the direction of the sprue bottom, because solidification must begin in the microparts and end in the bottom of the tree. On the one hand, this design is beneficial for good form filling; on the other, it helps to avoid shrinkage holes in the casting. This design rule, however, does not normally cause any problems in microcasting, because the parts are generally distinctly smaller than the feeder and runner system. Nonetheless, the heat capacity of the mold should also be taken into account because the compact molds used for microcasting show a comparatively high heat capacity. This results in the inner part of the massive form being still hot while the surface cools rapidly after the mold has been taken out of the furnace. Therefore, thin-walled parts should be positioned in the outer and thick-walled parts in the inner area of the mold. The melt will then remain liquid in the thick-walled parts for the longest time so that they can work as feeder for the thinner parts. As mentioned before, an adequate sprue system is necessary in order to avoid shrinkage holes in the thick-walled parts. More detailed information on the sprue design is given in the literature [37].

A special aspect in microcasting is the flow behavior in very fine channels. Owing to the much higher surface to volume ratio in microchannels compared with macrostructures and the distinct influence of surface roughness, the occurrence of turbulent flow needs to be taken into account. Another aspect is the extremely high cooling rate and therefore extremely fast solidification in the small structures, which hinders form filling much more than in macrostructures. This aspect will be discussed in more detail in Section 13.5.6.

13.2.1.3 **Melting**

For casting in different atmospheres, various set-ups are available. Some casting machines work with vacuum, some with air and others with an inert gas atmosphere. Also the furnaces can vary. There is electrical resistant heating, heating by an open flame, induction heating and melting by an arc furnace.

For resistance heating, the heat is produced by a heat winding which encloses the crucible. The heat winding can be made, for example, of platinum–rhodium. The method is used for alloys with casting temperatures up to about 1300 °C. Such set-ups with resistance heating are predominantly used for casting precious metals.

For the open flame technique, the metal is melted by a propane–oxygen flame in a ceramic crucible. The method is limited to relatively small amounts of metal and is especially used in dental casting workshops for heating high-melting

alloys to temperatures between 1300 and 1500 °C. Here, the use of a reducing flame is of great importance in order to eliminate oxides in the melt. The open flame technique requires good craftsmanship, but given this, good casting results can be achieved.

Induction heated casting machines allow for a higher automation level. They are now commonly used [38] in dental and jewelry casting because they exploit the widest range of casting atmospheres and temperatures. In induction heated equipment the metal is melted in a crucible surrounded by a water-cooled copper coil. An alternating current excites a magnetic field inducing eddy currents in the metal charge. This results in strong Joule heating due to the resistance of the charge carriers in the metal. The amount of energy injected depends on the alloy and the frequency (of the furnace). Modern equipment works with high frequencies in the region of 100 kHz. A benefit of this method is the very high melting rate. Owing to the direct injection of energy, higher melting alloys requiring casting temperatures above 1300 °C can be cast, compared with electrical resistance furnaces which are limited to 1300 °C in general. The induced eddy currents result in a strong convection in the melt. Hence good mixing and homogenization are achieved.

For melting with an arc flame, a pure argon atmosphere is necessary because the gas atoms work as charge carriers for the current flow. For the same reason, the metal to be molten must have electric contact with the crucible, which is normally connected as anode. The arc is then ignited between a tungsten cathode above the crucible and the crucible itself. Arc furnaces are very powerful and are also able to melt higher melting metals such as CoCrMo alloys or titanium.

The melting crucibles are made of ceramic or graphite. At high temperatures the graphite crucibles produce a reducing CO atmosphere as a result of the reaction of the carbon with the oxygen in the air. This is especially beneficial for precious metals because the melt is protected against oxidation. On the other hand, graphite crucibles tend to react with the melt so that for carbon-sensitive alloys ceramic crucibles are used normally. For titanium alloys, however, graphite crucibles are used although titanium is known to be a strong carbide former. In this case, a thin titanium carbide layer is formed in the crucible during the first melting process, which protects the melt during the following uses against reaction with the graphite crucible.

13.2.1.4 **Casting**

Metals to be processed by microcasting must have sufficient castability. The term embraces properties such as flowability and form filling ability, little contraction and shrinkage, reduced segregation, low porosity and shrinkage cavitation, little hot crack susceptibility, high surface quality and good mechanical properties. A metal is considered castable if the mentioned properties can be sufficiently achieved by using a given casting method. Based on the criteria form filling, surface quality, microstructure and dimensional accuracy, the cast-

ing quality can be judged. Deviations from the norm are regarded as casting defects. They originate either in faulty workmanship, in the selection of the wrong casting parameters or in limitations of the process. A typical problem is the solidification of the melt before the form is filled completely, which is a result of too low mold temperatures or insufficient overheating of the melt above the liquidus temperature. Additionally, incomplete casting can be caused by a filling pressure too low to overcome the surface tension of the melt, which is then unable to enter a cavity. Other important casting defects are described below. Shrinkage holes are a result of too fast solidification without sufficient feeding. Furthermore, so-called casting pearls may occur. These are metal pearls located on the casting due to primary air bubbles at the surface of the pattern which were not removed during embedding. Finally, surface shrinkage holes and surface pores caused by a too high casting temperature can sometimes be found in cast parts. Detailed information on casting defects and also images illustrating them can be found in the literature [39–42].

13.2.1.5 **Solidification**

The molten metal is poured into a preheated form distinctly cooler than the melt. The solidification starts with nucleation and crystal growth at the cooler mold wall [43]. At the same time, the volume of the melt decreases owing to the normal shrinkage process, which may then cause casting defects [39]. Therefore, it is important that the cast part solidifies first while the metal in the sprue still remains liquid. Another important aspect is the changing of the chemical composition during the solidification due to segregation. This segregation can occur in the center of cast blocks because companion elements and inclusions are pushed aside by the solidification front and accumulate in the rest of the melt. Graduated microsegregation inside dendrites or in general inside one phase, formed during solidification, also known as coring [43], is found in alloys which show a solidification interval. In this case, a difference in alloy composition between the center and the extremities of dendrite arms occurs owing to an enrichment of one element in the forming crystals at the expense of an impoverishment of the same element in the liquid. Alloys are prone to coring if the solidification is too fast to reach an equilibrium state according to the phase diagram [44]. The chemical composition can be homogenized by a subsequent long heat treatment at relatively high temperature.

13.2.2
Vacuum Pressure Casting

For vacuum pressure casting of microparts, dental casting machines can be used. Fig. 13-4 shows a scheme of the process. The metal is melted in the crucible located in the center of a heating winding. On top of the crucible the open mold is fixed upside down. After evacuation, the machine turns itself upside down (Fig. 13-4, right). As a result, the melt flows into the mold by gravity.

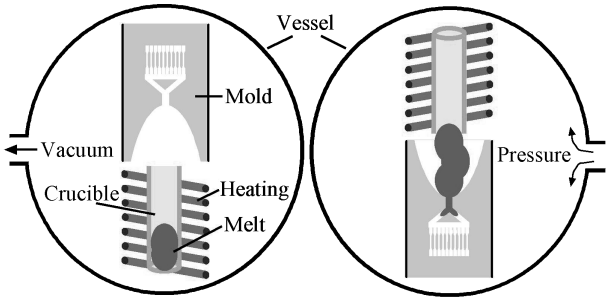

Fig. 13-4 Scheme of the vacuum pressure casting process. Left: vacuum condition with mold atop the heating chamber; right: pressure condition with melt discharged into the mold by force of gravity (machine turned upside down)

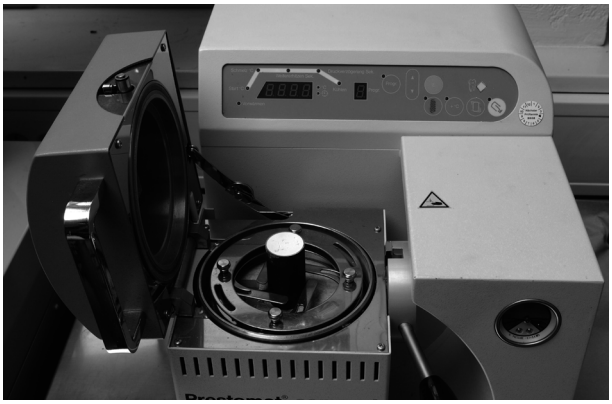

Fig. 13-5 Vacuum pressure casting machine Prestomat® by Degussa Dental GmbH

Complete form filling even of small cavities is achieved by subsequent application of pressure to the melt. Fig. 13-5 shows a view in the opened vacuum pressure casting machine Prestomat® from Degussa Dental GmbH. Vacuum pressure casting machines typically work at pressures of 3.5–4 bar, which is sufficient for the form filling of parts in the millimeter range. Depending on the special geometry of the microparts and the feeding system, this pressure may even be adequate for the casting of structures in the micrometer range. However, if extremely high aspect ratios are to be cast, a higher pressure is necessary. Calculations of the form filling behavior [45] show that the pressure which is necessary for the melt to enter an extremely small pinhole increases hyperbolically with decreasing radius. Neglecting several actual influences on the casting procedure, it was found that for fibers with a diameter of 1 µm a pressure of 20 bar is necessary to overcome the negative capillary forces which hinder the melt entering a small hole owing to the bad wetting behavior of the melt on

the mold. Considering real casting conditions, experiments showed that for parts with high aspect ratios, high pressure is beneficial even for parts with a diameter of 100 µm (see Section 13.5.6). However, it is very difficult to provide a pressure significantly higher than 4 bar because the pressure needs to be applied to the melt in a very short time interval t, where t ranges from 10^{-3} to 1 s. This means that a pressurized tank with a valve large in diameter is necessary to manage an immediate pressure increase.

On the other hand, a high pressure is not always desired because with increasing pressure the surface roughness determined by the generally porous investment increases owing to better replication of the surface structure of the mold. Therefore, an ideally flat mold surface without pores would be required, which, however, prevents residual air from leaving the mold during the form filling process.

13.2.3 Centrifugal Casting

In centrifugal casting, the mold rotates and the melt fills the mold by centrifugal forces. Fig. 13-6 shows a scheme of the process. The mold is fixed horizontally or nearly horizontally at one end of the centrifugal arm. On the other side, a counterweight is fixed to keep the balance of the rotation system. In most centrifugal casting machines the melt is first poured into the runner system and then the system starts to rotate, but there also exist some machines where the melt is poured into the already rotating system. Here the centrifugal forces are higher because the machine rotates already at top speed and no further acceleration has to be taken into account. The centrifugal casting machine Ticast® (Kobelco Research Institute, Inc.) shown in Fig. 13-7 is based on this principle [46]. Here, in contrast to the scheme in Fig. 13-6, the casting metal is melted in a crucible fixed midway above the centrifugal arm. When the melting process is finished, the crucible is tilted and the melt is poured into a so-called drop mold located exactly in the middle of the rotating system. From here the melt flow is directed into the rotating mold and fills the mold owing to centrifugal forces. The rotational speed of centrifugal casting machines is in the range 350–3000 rpm [48–50]. Modern centrifugal casting machines produce a higher pressure for form filling compared with vacuum pressure casting machines, which is beneficial for the casting of very small structures. However, the higher pres-

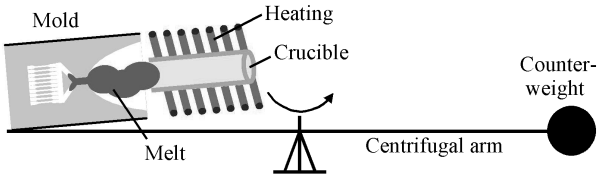

Fig. 13-6 Scheme of the centrifugal casting process

Fig. 13-7 Centrifugal casting machine Ticast® by Kobelco Research Institute, Inc.

sure can give rise to various defects in the casting and the high turbulences may cause gas entrapment and favors gas porosity [51]. This disadvantages need to be weighed against the partly significantly improved form filling (see Section 13.5.6).

13.2.4 Example of a Typical Casting Process

After assembling the micropatterns on a wax sprue, the investment is mixed. For phosphate bonded investments a mixing ratio of 100 g of powder and 14–23 ml of liquid is recommended [52]. With this mixture a total expansion of the mold between 1.2 and 2.4% can be achieved. It consists of the setting expansion due to chemical reactions in the investment and the thermal expansion during the heating (see Section 13.4.2). The expansion can be controlled additionally by the concentration of the liquid and can be varied in a wide range by adding distilled water to the liquid. Depending on the required mold size, powder amounts between 60 and 540 g are used in dental casting and in microcasting. The components are premixed manually for $\sim$30 s and then mixed for 60 s under vacuum. The processing time ranges between 4 and 6 min. During this time, the investment is poured into the cuvette containing the pattern assembly. The embedding process is supported by light vibrations using special equipment, for example Multivac® 4 by Degussa Dental GmbH. Subsequently the investment hardens for 20–50 min. According to the instructions for use in dental casting, the wax has to be eliminated in the next step by placing the mold in a preheated furnace at a temperature of about 300 °C. Depending on the mold size, this process takes between 30 and 60 min. Subsequently, the mold is transferred to another furnace for preheating with a starting temperature of 300 °C and is heated to the final temperature between 700 and about 1000 °C. Owing to the thermal expansion of the mold, a low heating rate of about 7 K/min is required. The final temperature needs to be held for about 20–60 min depending

on the mold size. Then the casting procedure begins with melting the alloy, for example in the vacuum pressure casting machine Prestomat® by Degussa Dental GmbH. Using Stabilor® G as casting alloy, the required amount of material (about 8–20 g) is melted at 1100 °C in a graphite crucible. After a 2 min dwell time, the preheated mold is placed in the machine and the casting process is started. Then the mold filled with the casting is removed, placed on a heat-resistant stone and is air-cooled. When the mold has reached ambient temperature, it is removed and the cast structure is cleaned in hydrofluoric acid and then washed in water. Finally, the microcomponents are separated from the runner and sprue.

13.3 Casting Alloys

13.3.1 Introduction

Although, in theory, all meltable metals can be cast, the casting suitability of alloys differs significantly. This is particularly important for microcasting, because here extremely small structures need to be filled sufficiently. Therefore, the most relevant factors for a casting alloy are high form filling ability and flowability of the melt. They are influenced by the viscosity of the melt, the wetting behavior of the form, the reaction with the mold and the atmosphere and, of course, by the solidification behavior. A high form filling ability and a good flowability are mainly guaranteed for precious alloys such as are used in jewelry and dental casting, for bronze (handcraft arts) and for high-strength alloys, such as CoCrMo alloys, which are especially used for dental castings. Steels are not widespread in microcasting because of their oxidation and corrosion sensitivity.

13.3.2 Gold Base Alloy as an Example of Precious Metals

In ancient times, precious alloys, especially gold and gold alloys, were used for casting small structures. The earliest example of a lost wax casting in gold alloy is a small animal figure on the rein-ring from Queen Pu-Abi's chariot dated about 2600 BC [53, 54]. Further examples were recovered on the Greek islands, in Anatolia, in Mesopotamia and in the vicinity of the Dead Sea [54–56]. The gold coffin treasures of the Egyptians also include cast parts made by the lost-wax method. The historical knowledge of forming gold by investment casting has now been rediscovered for the manufacturing of microparts.

The advantage of gold and gold base alloys is their relatively low melting and casting temperatures. These materials are known to have excellent castability and a low oxidation affinity during the casting process. Because of their color and their high resistance against corrosion and tarnishing, gold and gold base

alloys are eligible materials for jewelry. Good chemical properties and biocompatibility are essential for all materials used in oral health applications. Furthermore, sufficient mechanical properties regarding the service stresses are required [57]. For the fabrication of crowns and bridges, mainly alloys based on the ternary system AuAgCu are used. The increase in strength achievable compared with pure gold depends on the composition and the aging temperature. Scientific investigations of ternary AuAgCu alloys have shown a complex combination of constituent age-hardening mechanisms such as ordering processes of the CuAu I phase, precipitation and spinodal decomposition [58–60]. Similar results are documented for several commercial low-carat gold alloys for dental applications often containing Pd and some additional elements in minor amounts [61–63].

Owing to the good castability and high mechanical strength, an age-hardening gold base alloy was the first choice for research and development of microcasting based on investment casting. Especially the good casting properties recommended this material for replicating turbine parts with 10–30 μm wall thickness and specimens for mechanical testing with an aspect ratio (flow length-to-wall thickness ratio) up to about 30. Previous investigations led to the choice of the gold base dental alloy Stabilor® G, manufactured by Degussa Dental GmbH. Like the other age-hardening materials mentioned before, Stabilor® G is based on the ternary system AuAgCu and, therefore, shows good chemical resistance combined with excellent mechanical properties. It is especially suited for devices in mechanical engineering. Detailed specifications of this alloy concerning the chemical composition and the mechanical properties given by the supplier Degussa Dental GmbH are presented in Tables 13-1 and 13-2. The melting range is between 860 and 940 °C.

Table 13-1 Composition of Stabilor® G in wt.% (values given by manufacturer)

Au	Ag	Cu	Pd	Zn	Pt	Ir
58.0	23.3	12.0	5.5	1.0	0.1	0.1

Table 13-2 Mechanical properties of Stabilor® G (values given by manufacturer)

Condition	Yield stress (MPa)	Ultimate tensile strength (MPa)	Hardness HV5	Elongation to fracture (%)
As quenched	400	510	170	33
Precipitation hardened	830	890	275	6

13.3.3
Bronze as an Example of Typical Casting Alloys

Other typical casting alloys such as bronzes, with 5–12 wt.% aluminum as primary alloying element, are especially used for corrosion-resistant castings because they form a thin oxide surface layer which protects the alloy against corrosion. In addition to aluminum, these alloys often contain iron, nickel or manganese in order to improve their mechanical properties. Commercial alloys based on such compositions rank among the best acid-resistant high-strength alloys [64]. Al-bronzes are excellent wear-resistant materials and are, therefore, used in gears, bearings, bushes etc. [65].

The microstructure of Al-bronzes depends mainly on the alloying elements and the cooling rate. Additionally, further microstructural changes occur during subsequent heat treatment. Benkisser et al. [66], for example, explained in detail the microstructure of a cast CuAl10FeNi alloy that underwent slow cooling.

Faster cooling, however, results in non-equilibrium phases. In this context, Horn-Samodelkin et al. reported the presence of a martensitic phase in a sand cast plate of G-CuAl10Ni [67]. For the binary system Cu–Al, Fig. 13-8 shows a transition diagram [68] with both the equilibrium phases and the transition temperatures for order and martensitic transformations. After solution heat treatment in the β-region and subsequent quenching in water, the β-phase still exists at ambient temperature. During quenching, the alloy passes two through order transformations and later forms martensite. The modification of the martensite phase depends on the Al content of the alloy. Additionally, three different martensites, α', β_1' and γ', can be distinguished by their crystal structures.

The advantage of Al-bronze for microcasting is the formation of a thin, transparent oxide layer, which already gives the casting a metal brightness without any chemical cleaning or mechanical polishing. Furthermore, compared with Sn-bronze, Al-bronze has a narrow solidification interval between 1020 and 1040 °C, which limits the tendency to segregate during solidification. Like Al-

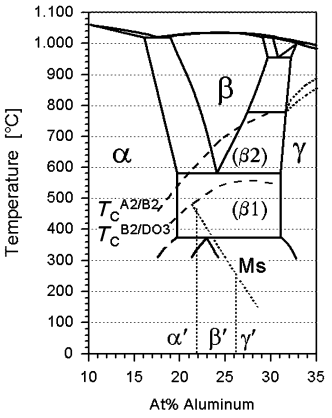

Fig. 13-8 Transition diagram for binary CuAl alloys. Continuous line, phase diagram; dashed line, transition temperatures of order transformations and martensite formation. Adapted from Kainuma et al. [68]

Table 13-3 Composition of Al-bronze in wt.% (according to DIN 1714)

Cu	Al	Ni	Fe
76	8.5–11.0	4.0–6.5	3.5–5.5

Table 13-4 Mechanical properties of Al-bronze (according to DIN 1714)

Yield stress (MPa)	Ultimate tensile strength (MPa)	Hardness HV5	Elongation to fracture (%)
270–300	600–700	140–160	12–14

bronzes, the CuAl10Ni alloy used for our investigations shows generally good mechanical properties and good slip properties and is resistant against sea water. The chemical composition and the mechanical properties according to DIN 1714 are shown in Tables 13-3 and 13-4.

13.3.4 CoCrMo Alloy as an Example of High Strength Materials

CoCrMo alloys are well-known alloys in medical and dental applications. Especially in surgical implant applications, Co-base alloys are used as materials for the reconstruction of artificial joints because of their good mechanical properties and their excellent corrosion and biodegradation resistance. In dental techniques, CoCrMo alloys are mainly used for casting dentures. The high ultimate tensile and fatigue strength of the alloy combined with a sufficient elongation at fracture are of great importance [69]. CoCrMo alloys also guarantee biocompatibility, which means that the material itself remains unchanged by body liquids and does not interact unfavorably with body tissue [70]. The superior corrosion resistance is due to the fact that alloys with high chromium content form a passive oxide layer on the surface, protecting the alloy against the environment of the body. Cast CoCrMo alloys are known to exhibit an inhomogeneous, large-grained microstructure [71]. SEM and TEM investigations showed that the apparent two-phase microstructure seen in optical microscopy consists of many more phases. Investigations of a cobalt base alloy with 0.4% C, 30% Cr and 5% Mo, using energy-filtered TEM, proved the existence of an extremely fine ternary eutectic additionally to a blocky σ-phase [72]. According to Kulmburg et al., it consists of a cobalt-rich solid solution, $M_{23}C_6$- and M_6C-carbides. The extremely fine ternary eutectic is thought to be the reason for the good casting properties of the material. Other groups investigating a Co base alloy with 27.0–30.0% Cr, 5.0–7.0% Mo and maximum 1.0% Ni, 0.75% Fe, 0.35% C, 1.0% Si and 1.0% Mn found cobalt-rich dendrites and an interdentritic four-phase mixture containing a cobalt-rich γ-phase, a chromium-rich $M_{23}C_6$ phase (with M = Co, Cr or Mo), an M_7C_6 phase and a chromium and molybdenum-rich σ-phase [73, 74].

Table 13-5 Mechanical properties of Biosil® f (values given by manufacturer)

Yield stress (MPa)	Ultimate tensile strength (MPa)	Hardness HV10	Elongation to fracture (%)	Young's modulus (GPa)
700	900	400	5	220

Table 13-6 Composition of Biosil® f in wt.% (values given by manufacturer)

Co	Cr	Mo	Si	Mn	C
64.8	28.5	5.3	0.5	0.5	0.4

Often these interdendritic phases reduce the ductility and the corrosion resistance and also limit the strength. Therefore, a subsequent solution heat treatment is recommended for cast CoCrMo alloys. According to Clemow and Daniell [73], the optimum temperature for this is 1225 °C. Exact temperature control during heat treatment is of great importance because the annealing needs to be kept below the eutectic temperature of 1235 °C in the CoCrMo system. According to Sullivan et al. [75], for CoCrMo alloys a yield stress of at least 450 MPa, an ultimate tensile strength of 655 MPa and an elongation at fracture of 8% can be expected. Interdendritic porosity, often found in cast CoCrMo alloys, is detrimental to the mechanical properties.

The dental CoCrMo alloy Biosil® f used for microcasting reaches a nominal yield stress of 700 MPa, an ultimate tensile strength of 900 MPa and an elongation at fracture of 5% according to the manufacturer (Table 13-5). The exact chemical composition of the alloy is given in Table 13-6. The melting temperature of the alloy lies between 1320 and 1380 °C. The recommended preheating temperature for this alloy is 1000 °C and the recommended casting temperature 1500 °C [76]. During casting, a passivation layer is formed on the surface which should not be destroyed. Therefore, the cast part should not be treated with a stripping agent [76].

13.4 Investment Materials

13.4.1 Introduction

The investment is a ceramic slurry in which the pattern is embedded to produce a mold for casting. It has a significant influence on the casting result and should therefore meet several requirements. For embedding purposes, the investment should have good flowability and processibility. After drying, further

burning at increasing temperatures is necessary in order to guarantee the required mechanical and thermal stability. The resulting mold should be chemically inert with regard to the metal melt, and furthermore it should show an adequate dimensional behavior, sufficient mechanical strength and low surface roughness and porosity [77]. At the end of the casting process, easy removal of the mold from the cast part is desirable.

The investment is a mixture of a binder and a filler, with the binder itself consisting of powder and liquid. The solidification of the investment is facilitated by a chemical reaction of the binder components which results in stable inorganic phases. Most common binder materials used in dental and jewelry casting are slurries or liquids based on phosphate, plaster or silicate. For the shell casting technique, which is mainly applied for macroparts, often binders on a silicate base are used. Fillers are in all cases ceramic powders. Typical minerals used as fillers in investments are quartz, cristobalite, aluminum oxide, zirconium oxide, zirconium silicate and burned potter's clay minerals such as mullite and molochite. In dental techniques, the filler materials mainly used are quartz and cristobalite, which are both modifications of SiO_2. Additionally, for investment casting, the amorphous modification of SiO_2 named melt quartz or amorphous quartz is used.

The special importance of the minerals quartz and cristobalite lies in their high thermal expansion behavior. In contrast to amorphous quartz, these minerals show phase transitions which are associated with a strong volume increase. The transition from low- to high-temperature quartz at 573 °C results in a volume increase of 0.8%. Cristobalite, which at ambient temperature has a 14 times higher specific volume than quartz, shows a volume increase of 2.8% on transforming from the low- to high-temperature form at a transition temperature of 270 °C [78]. Owing to kinetic effects, impurities and mismatches in the crystal structure of the raw material, the real values of the volume increase may differ from the values given in the literature.

Fig. 13-9 compares the linear thermal expansion of the three SiO_2 modifications quartz, cristobalite and amorphous quartz [79]. Here, cristobalite shows a sudden change from the low- to the high-temperature modification in the vicinity of the transition temperature ($\sim$270 °C). The total linear thermal expansion of cristobalite is 1.6% for temperatures up to 800 °C. However, quartz expands by 1.3% up to temperatures of about 650 °C, whereas at higher temperatures a contraction is observed. The thermal expansion of amorphous quartz is very low, $<$0.1%. Hence the expansion behavior of the investment during heating to standard mold temperatures between about 700 and 1000 °C is mainly controlled by its cristobalite and quartz content. With increasing cristobalite content, the expansion of the investment increases.

For high-precision replication, good contour accuracy is required in addition. This is guaranteed by special fine-scaled investments. However, excessive downscaling of the filler particle size is problematic, because the increasing particle surface requires a higher liquid content. This results especially for phosphate bonded investments in drying cracks during hardening. For plaster bonded in-

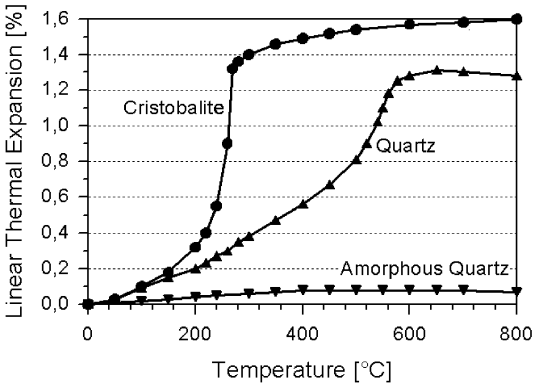

Fig. 13-9 Linear thermal expansion of quartz, cristobalite and amorphous quartz. Adapted from Degussa Dental GmbH [79]

vestments, however, the amount of water can be varied over a wider range without inducing cracks, but it has to be stressed that an increasing water content in the investment hampers the drying process [17].

13.4.2 Phosphate Bonded Investments

The choice of the investment material depends on the cast metal and the required strength of the mold. Phosphate bonded investments were initially used for dental alloys with a high melting temperature at casting temperatures between 1200 and 1500 °C. However, in dental casting, these investments are nowadays used for all alloys because of their high heat resistance, good mechanical strength and convenient workability. They consist of magnesium oxide and ammonium hydrogenphosphate as binder and the two different SiO_2 modifications quartz and cristobalite as filler. Special investments for gold base alloys sometimes also contain graphite powder in order to produce a reducing atmosphere in the mold. The powdery binder and filler components are mixed with a liquid which mainly consists of aqueous silica sol. The water content in the liquid is necessary to facilitate a chemical reaction [80]:

$$NH_4H_2PO_4 + MgO + 5H_2O \quad \rightarrow \quad MgNH_4PO_4 \cdot 6H_2O$$

In the burning process, ammonium phosphate is converted into magnesium pyrophosphate, releasing water and ammonia according to [80]

$$MgNH_4PO_4 \cdot 6H_2O \quad \rightarrow \quad MgNH_4PO_4 \cdot H_2O + 5H_2O \qquad > 160^\circ C$$

$$2(MgNH_4PO_4 \cdot H_2O) \quad \rightarrow \quad Mg_2P_2O_7 + 3H_2O + 2NH_3 \qquad > 250^\circ C$$

Above 1000 °C the investment decomposes by continuous reaction of excrescent magnesium oxide with the phosphate of the binder and the silicate of the filler [80]:

$$Mg_2P_2O_7 + MgO \rightarrow Mg_3(PO_4)_2 \quad > 1000°C$$

$$2MgO + SiO_2 \rightarrow Mg_2SiO_4 \quad > 1000°C$$

Commercial investments for dental casting are designed in such a way that they exactly compensate the shrinkage of a given metal during solidification. During the manufacturing process, the necessary expansion of the investment is mainly achieved by the expansion of the filler due to the change from a low- to a high-temperature phase (cristobalite, 270 °C; quartz, 573 °C; see Fig. 13-10), which comprises a modification of the crystal structure. To allow enough time for the phase transitions, a slow heating regime is required in order to avoid cracks. Degussa Dental GmbH recommends a heating rate of 7 K/min for several of their phosphate bonded investments [52].

The thermal and chemical expansion of the binder is controlled by the silica sol concentration of the liquid and generally increases with increasing concentration of the liquid (Fig. 13-10). Additionally, the amount of silica sol determines the surface roughness of the mold because it transforms into amorphous SiO_2 during burning and fills the pores of the mold. Whereas silica sol reduces the porosity of the mold, adding graphite increases it. Graphite-containing investments are used for better gas permeablity of the mold and easier deflasking of the cast parts.

Phosphate bonded investments have a higher strength than plaster bonded investments [81] and are more convenient to handle. Hence they are widespread in dental laboratories for precious metals and for model casting alloys on a

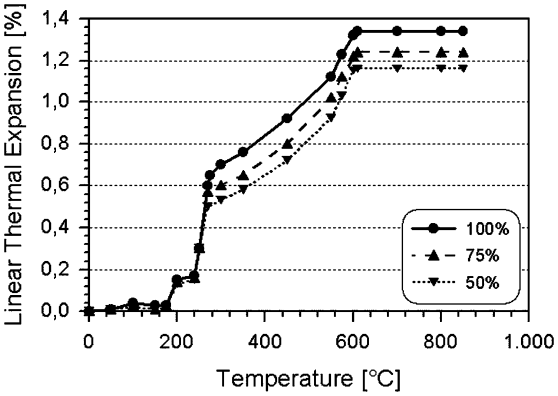

Fig. 13-10 Thermal expansion behavior of phosphate bonded investment. Adapted from Degussa Dental GmbH [79]

CoCr base. For the latter, additionally the higher possible preheating temperatures up to 1000 °C are important.

13.4.3 Plaster Bonded Investments

When casting microparts, a great difficulty is the removal of the investment. For gold base alloys, phosphate bonded investment can be removed by acid owing to the higher chemical resistance of the metal compared with the investment, but for base alloys such as bronze or CoCrMo alloys this procedure is not applicable. Hence special investments which are easily soluble are required. This is achieved by using plaster as binder. Like phosphate bonded investments, plaster bonded investments contain quartz and cristobalite as refractory filler materials. Additionally, the investments often contain auxiliary materials. The material is commonly employed in casting gold alloys with high gold content and with liquidus temperatures not higher than 1080 °C [81]. In dental applications, plaster bonded investments are not used as often as in jewelry casting owing to the danger of sulfur release by reactions of the melt with the investment and hence resulting low strength of the casting. In jewelry and artistic casting, however, most investments are plaster based, because they achieve a low surface roughness and can be easily removed also from complicated-shaped structures. Plaster used in investments is hard plaster or super-hard plaster, chemically both α-semihydrates. For cuvette embeddings, hard plaster can be used, but if precision and high mechanical strength are required then super-hard plaster should be adopted [82]. When mixing the slurry for embedding, the chemical reaction of α-semihydrate with water results in calcium sulfate dihydrate [83]:

$$CaSO_4 \cdot \frac{1}{2}H_2O + \frac{3}{2}H_2O \quad \rightarrow \quad CaSO_4 \cdot 2H_2O$$

This rehydration is an exothermic process. Stoichiometrically, 18.7 ml of water are needed to rehydrate 100 g of plaster, but for mixing a well-flowing slurry for embedding additional water is required [82]. Depending on the particle size and form of the crystals, 100 g of α-semihydrates need 28–32 or 19–29 ml of water, respectively, depending on the modification hard plaster or super-hard plaster. During burning, the crystal water is released and the anhydrite of calcium sulfate for the mold is obtained [79]:

$$CaSO_4 \cdot 2H_2O \quad \rightarrow \quad CaSO_4 + 2H_2O$$

Above 750 °C, calcium sulfate decomposes according to [79]

$$2CaSO_4 \quad \rightarrow \quad 2CaO + 2SO_2 + O_2$$

The generation of sulfur dioxide may result in deterioration of the casting due to gas bubbles in the near-surface region if the gas cannot be dissipated

through the porous mold. Another problem with plaster bonded investments is the decomposition of the investment between 500 and 600 °C if carbon is present [79]:

$$CaSO_4 + 4C \rightarrow CaS + 2CO_2$$

During setting, the plaster shows a change in volume. Although the real volume will decrease by 7% when the starting substances are mixed together, the apparent volume will increase owing to the feeding by the slurry during the solidification of the mold. The volume change is determined by the linear difference in elongation. For dental plasters, first a linear contraction is found followed by a linear setting expansion between 0.05 and 0.15% for special hard plasters [82].

13.4.4 Influence of the Investment on the Surface Roughness

The investment has a significant influence on the surface roughness of the cast part. With increasing form filling ability of the casting alloy, the surface roughness of the cast part approaches more and more that of the surface of the mold. Therefore, a very smooth surface of the mold with only a few pores is necessary. Three different ways are possible to meet these requirements:

- coating the pattern with an extremely fine ceramic;
- infiltrating the sintered mold with a ceramic suspension; and
- modifying the investment by addition of fine ceramic particles [84].

Within the scope of the Collaborative Research Center 499 [85], comparative roughness measurements were made employing the three methods mentioned above. The surface topography of the cast parts, which replaced or replicated a smooth, injection-molded PMMA plate 4×6 mm^2 in size, was imaged by a tactile system (Perthometer®, Mahr GmbH) with a tip radius of the needle of about 1.4 µm and a load between 10^{-3} and 10^{-5} N. The roughness values R_a and R_{max} were calculated along a 5.6 mm long segment on the plain side of each sample. R_a is the arithmetic mean of the deviations of the absolute values with respect to the center line of the roughness profile [86–88]. R_{max} is defined as the largest single deviation from peak to valley along the measured segment. The surface roughness of the ceramic mold was determined by a contactless, optical-measuring system (Microglider®, Fries Research & Technology GmbH) because the mold is too weak to withstand a tactile system.

In the following, the three different methods for reducing the surface roughness of the ceramic mold and therefore of the cast part will be described.

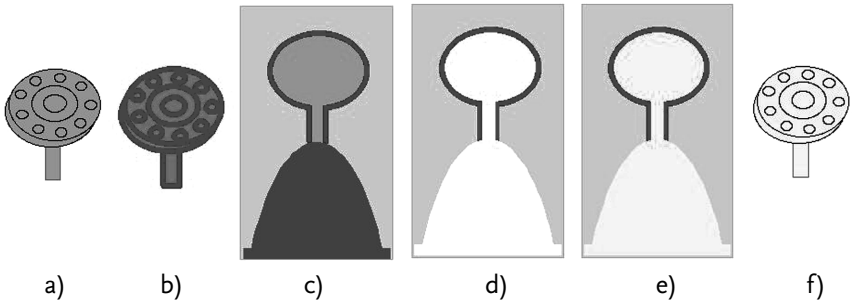

Fig. 13-11 Sketch of casting process with coated pattern.
a) PMMA pattern; b) coated pattern; c) coated pattern in ceramic slip;
d) hollow form after sintering with coating left inside the mold;
e) metal-filled form; f) cast part

13.4.4.1 **Coating the Pattern**

Investigations on surfaces improved by coating the pattern were carried out with a 1% aqueous methylcellulose solution containing 5% fine-scale SiO_2 powder. The pattern was dipped into the liquid and dried on air. Subsequently, the coated pattern was embedded in an investment slip (Deguvest® CF by Degussa Dental GmbH), dried and burned as described before. The hollow form was then filled with the molten gold base alloy Stabilor® G in a vacuum pressure cast machine (Prestomat® by Degussa Dental GmbH). The applied pressure was 4 bar. A sketch of the process is given in Fig. 13-11.

The profile for surface roughness for cast parts that were replicated in the commercial investment shows large amplitudes with roughness values of $R_a = 1.13$ µm and $R_{max} = 8.41$ µm whereas a coated specimen achieves values of only $R_a = 0.74$ µm and $R_{max} = 6.19$ µm. Therefore, coating of the mold is beneficial to a low surface roughness of the cast part. However, it must be stressed that coating a plastic or wax pattern is difficult owing to the poor adhesion of the liquid on the pattern. Dipping the PMMA pattern in the slurry once leads to a coating which delivers relatively good results. Repeated dipping two or three times, however, often results in flaking of the coating.

13.4.4.2 **Infiltrating the Mold**

Infiltration was examined using suspensions of fine-grained SiO_2 powder stired in distilled water (1:10). In further experiments it was diluted to 1:20 and 1:40. The process of infiltration is illustrated in Fig. 13-12. First the mold was manufactured as discussed earlier. The hollow form was then infiltrated with the suspension and sintered in a second burning process followed by the final casting process.

Compared with the coating technique, the infiltration of a microstructured sintered form is much more difficult. If the viscosity of the suspension is too high, it does not infiltrate the pores of the mold but instead forms a thick layer

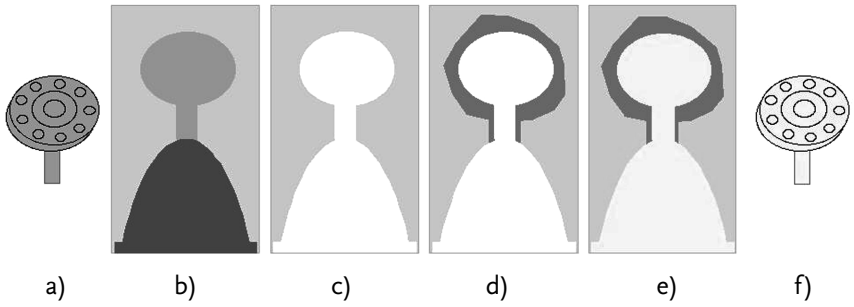

Fig. 13-12 Sketch of casting process with infiltration.
a) PMMA pattern; b) embedded in ceramic slip; c) hollow form;
d) infiltrated investment after second sintering; e) metal-filled form;
f) cast part

on the surface, leading to rounded edges and differences in tolerance. However, when the viscosity of the infiltration liquid is too low, then there is no visible effect on the mold. It fully penetrates the porous investment without leaving a layer on the mold surface. Additional investigations showed that it is almost impossible to realize a homogeneous infiltration in a closed mold with internal microstructures. Appropriate tests for this technique proved inconclusive.

13.4.4.3 **Modifying the Investment**

Reduction of the surface roughness is also possible by modifying the investment compound itself. Therefore, different amounts of fine-grained SiO_2 powder were added to the Deguvest investment. To maintain the consistency of the slip, the liquid content was increased at the same time. The modifications used are summarized in Table 13-7.

When the commercial investment (Deguvest® CF) was modified, much better results than with the first two methods were achieved. Compared with the commercial investment, modification 1 results in a slightly lower R_a value, but in an increased R_{max} value for the cast parts (Table 13-8). The second modification, however, achieves a significant reduction in both surface roughness values (Table 13-8). The R_a value decreases from 1.13 µm for the commercial investment to 0.44 µm for modification 2 and at the same time the R_{max} value decreases from 8.41 to 3.24 µm.

Table 13-7 Composition of the investment modifications used

	Modification 1	**Modification 2**	**Modification 3**
Deguvest® CF	60 g	60 g	60 g
SiO_2 powder	12 g	12 g	8 g
Liquid	10 ml water + 30 ml liquid	40 ml	29 ml

Table 13-8 Influence of investment on the roughness of cast surfaces

Investment	R_a (µm)	R_{max} (µm)
Commercial investment	1.13	8.41
Modification 1	0.97	10.74
Modification 2	0.44	3.24

The lower surface roughness of the parts cast in modified investment originates in a reduction of the pore size in the mold [84] owing to the use of a larger amount of fine-grained filler in the investment. However, there will be a limitation to this development owing to the necessity for an open porosity in the mold in order to allow the exit of gas out of the cavities during the form filling process. Another problem when using fine-grained investment is the increasing demand for liquid for mixing the slurry owing to the large surface area of the fine-grained powder that needs to be wetted. The high liquid content in the investment often causes cracks in the mold during drying and burning.

13.5 Cast Microparts and Their Properties

13.5.1 Examples of Cast Microparts

Within the scope of this research, a wide variety of microparts were cast, including specimens for mechanical testing (bending bars, tensile test specimens) and parts for a demonstrator consisting of a turbine and a gear unit. Fig. 13-13 (left) displays an array of bending bars with a geometry of $200\times200\times1800\ \mu m^3$ each.

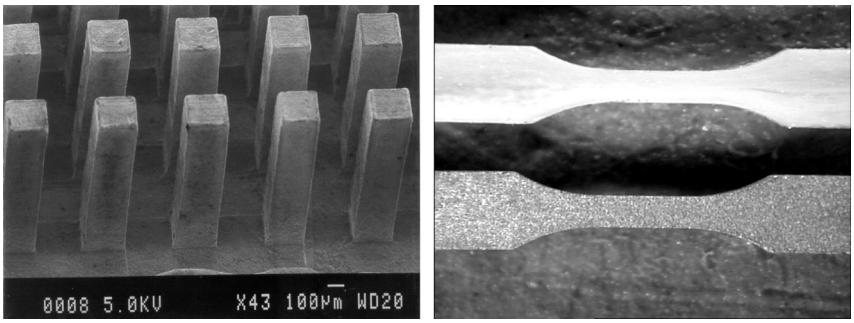

Fig. 13-13 Specimens for mechanical testing cast in gold base alloy Stabilor® G. Left: bending bars ($200\times200\times1800\ \mu m^3$); right, tensile test specimens ($260\times130\times4000\ \mu m^3$) (top: plastic pattern; bottom: cast part)

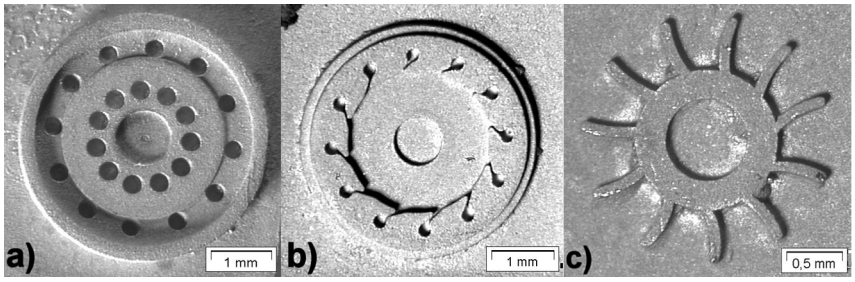

Fig. 13-14 Turbine parts cast in gold base alloy. a) Housing; b) nozzle plate; c) (blade) wheel

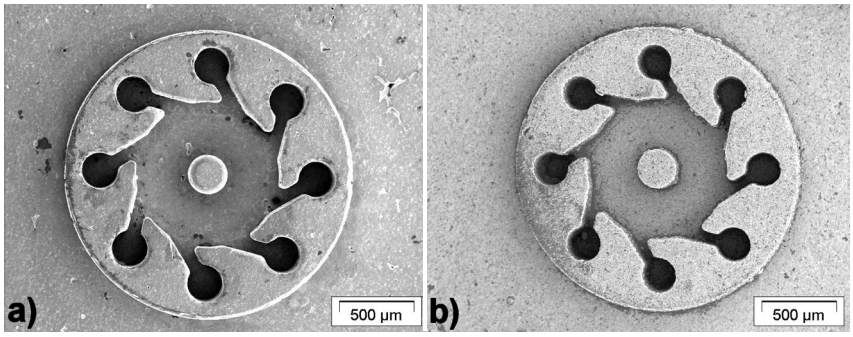

Fig. 13-15 Cast turbine parts made of different alloys. a) Al-bronze; b) CoCrMo alloy

On the right, a tensile test specimen with a total length of 4 mm and a rectangular cross-section of $130 \times 260\ \mu m^2$ in the gage length is shown below the plastic pattern used as a model. The discussed specimens for mechanical testing are both made of Stabilor® G.

In addition, microparts for a demonstrator consisting of a turbine with a diameter of 4 mm and a gear unit were cast in the gold base alloy Stabilor® G. The smallest geometry can be found on the nozzle plate (Fig. 13-14 b) with a channel width of 25 µm and a channel height of 200 µm. The blades of the wheel (Fig. 13-14 c) have a thickness of 100 µm, a length of about 400 µm and a structural height of 190 µm. The housing (Fig. 13-14 a) has holes with a diameter of 200 µm in the outer circle and 210 µm in the inner circle. The entire height of the housing is about 395 µm and 245 µm in the inner area where the nozzles are located. The dimensional accuracy is discussed in Section 13.5.3.

Additionally to the gold base alloy, a bronze and a CoCrMo alloy have been used to cast microturbine parts. Fig. 13-15 shows corresponding nozzle plates with an outer diameter of 1.9 mm. The channel width is 75 µm and the height is 350 µm. The nozzles themselves have a diameter of 200 µm.

13.5.2 Microstructure/Grain Size

The microstructure of cast parts is mainly influenced by the mold temperature. An increase in the mold temperature directly lowers the cooling rate. For a quantitative investigation, wax sticks with a diameter of 3 mm were equipped with three thermocouples each: one near the sprue bottom (TC 1), one in the middle (TC 2) and one at the top of the stick (TC 3). A single wax stick carrying the thermocouples was then embedded in an investment. After heating to 700 °C, the mold was kept constantly at this temperature. This process was repeated with a second wax stick–investment combination that was allowed to cool after burning and then kept at 100 °C for 1 h. Later, both molds were filled with the gold base alloy Stabilor® G using a casting temperature of 1100 °C. Fig. 13-16 shows the time-dependent temperature development in the mold during casting. The cooling rate is highest at the beginning of the casting process. The temperature for a mold that was kept at constant 700 °C (Fig. 13-16 b) decreases by only 150 °C within the first 20 s, whereas for a mold held at 100 °C (Fig. 13-16 a) a much higher cooling rate is observed. Grain size analyses of the above sticks show a significant influence of the mold temperature on the average grain size (Table 13-9). The grain size increases from 24 µm for a mold tem-

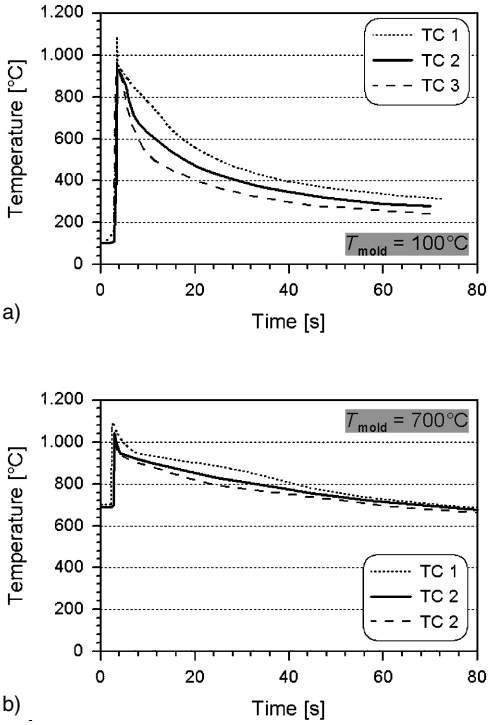

Fig. 13-16 Influence of two mold temperatures on the temperature development in a cast stick made of gold base alloy Stabilor® G with a diameter of 3 mm. (a) Mold temperature 100 °C; (b) mold temperature 700 °C. TC 1, thermocouple at the gate; TC 2, thermocouple in the middle of the stick; TC 3, thermocouple at the top end

Table 13-9 Influence of mold temperature on grain size for sticks of 3 mm diameter cast in the gold base alloy Stabilor® G

Mold temperature (°C)	Grain size (µm)
100	24
400	35
700	56
1000	91

Table 13-10 Influence of mold temperature on grain size for sticks of 3 mm diameter cast in Al-bronze

Mold temperature (°C)	Grain size (µm)
100	~30
400	~45
700	~100
1000	~170

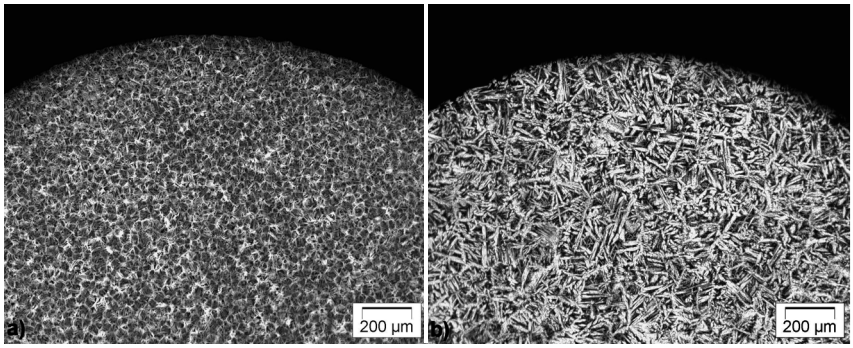

Fig. 13-17 Influence of mold temperature on the microstructure for sticks with 3 mm diameter cast in Al-bronze. a) Mold temperature 100°C; b) mold temperature 1000°C

perature of 100°C up to 91 µm at 1000°C. However, while a stick diameter of 3 mm is still a macrosize, smaller grain sizes have been found for microstructures (see examples in Chapter 19). They generally underlie higher cooling rates as a result of the smaller amount of heat induced in the mold during casting. The influence of the mold temperature will increase with decreasing structure size because the influence of the heat content of the mold increases relative to the heat content of the cast part [37]. In addition to the grain size, the cooling rate also influences the precipitation behavior of hardened alloys such as Stabilor® G because with an increasing cooling rate the solidification turns more and more into a quenching process far away from any metallurgical equilib-

rium. Therefore, when using low mold temperatures a subsequent annealing process is recommended in order to achieve an adequate age-hardened microstructure.

The effect of the mold temperature or cooling rate on the grain size of Al-bronze is shown in Table 13-10. This material, in comparison with the gold alloy (Table 13-9), exhibits distinctly coarser grain sizes. For cast sticks with a diameter of 3 mm, the grain size increases from about 30 µm for a mold temperature of 100 °C up to about 170 µm at 1000 °C. Additionally, cross-sections of the Al-bronze sticks in Fig. 13-17 show an obvious coarsening of the different phases with increasing mold temperature from 100 to 1000 °C.

13.5.3 Dimensional Accuracy

In the microcasting process, very good dimensional accuracy can be achieved when using an investment which is in compliance with a casting metal regarding the expansion behavior. In order to determine the dimensional accuracy of the casting process, an array of 144 vertical bending bars was embedded in Deguvest® CF, the investment for gold base alloys supplied by Degussa Dental GmbH and replicated with Stabilor® G as corresponding metal. In contrast to the standard microcasting process, a wax pattern replicated (via silicon) from a milled brass array was used. Fig. 13-18 shows the mean width of the bending bars for the original made of brass, for the wax pattern and for the cast parts averaged over about 100 specimens each. The original, with 209.2 µm, is distinctly larger than the nominal value (200.0 µm). The size of the replications decreases slightly from the wax pattern (207.8 µm) to the cast bending bars (206.3 µm). For the precision of the casting process, however, only the dimensional accuracy of the cast parts compared with the wax pattern is of interest. As the standard deviations are similar at 4.2 and 3.9 µm, respectively, it is therefore possible to compare the values for the mean widths. In the given example, the difference is only 1.5 µm, which is within the accuracy of measurement. This value displays a very good dimensional accuracy of the casting process.

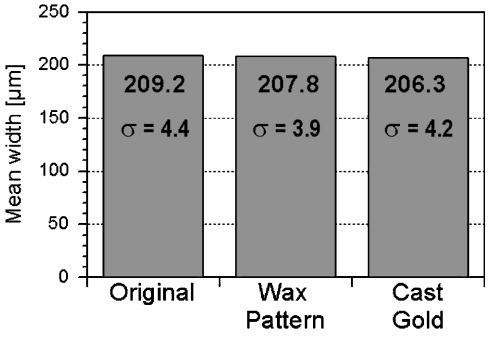

Fig. 13-18 Dimensional accuracy of cast parts made of Stabilor® G bending bars 200×200×1800 µm³ cast as array of 144 specimens at a mold temperature of 700 °C. Shown is the mean width and the standard deviation σ of the original, the wax patterns and the cast part; all values given in µm

13.5.4 Surface Roughness

The surface roughness is influenced by various parameters. One parameter is the investment, as discussed in Section 13.4.4; the two other important parameters are the mold temperature and the casting pressure. The influence of these parameters was measured on tensile test specimens made of the gold base alloy Stabilor® G using both a confocal white light microscope (NanoFocus µSurf NanoFocus AG) and a scanning optical system (Microglider®, Fries Research & Technology GmbH). Both set-ups are contactless measuring systems. The measuring lengths are comparable and lie between 1.2 and 1.6 mm. Tables 13-11 and 13-12 present the roughness values R_t and R_z measured by NanoFocus and R_a and R_z measured by FRT for specimens cast under different conditions. Comparing specimens cast at a mold temperature of 1000 °C but with different casting techniques, it can be seen that the surface roughness achieved by vacuum pressure casting is significantly lower than that by centrifugal casting. This is due to the different filling pressures applied in the two methods. Whereas the centrifugal casting machine works with a filling pressure of about 20–25 bar, the vacuum pressure casting machine fills the mold with only 4 bar. This results in a different quality of replication of the surface roughness of the mold. The high pressure in the centrifugal casting machine leads to a better replication of the mold surface but at the same time results in a higher surface rough-

Table 13-11 R_t and R_z values measured with NanoFocus [89]. CC: centrifugal casting; VPC: vacuum pressure casting; measuring length: ~1.6 mm

Mold temperature (°C)	Casting technique	No. of specimens	R_t (µm)		R_z (µm)	
			Mean value	Standard deviation	Mean value	Standard deviation
700	CC	63	9.53	4.51	5.96	3.13
1000	CC	36	8.68	3.82	5.34	2.63
1000	VPC	11	4.19	0.50	2.85	0.27

Table 13-12 R_a and R_z values measured with FRT. CC: centrifugal casting; VPC: vacuum pressure casting; measuring length: 1.2–1.5 mm

Mold temperature (°C)	Casting technique	No. of specimens	R_t (µm)		R_z (µm)	
			Mean value	Standard deviation	Mean value	Standard deviation
700	CC	6	1.35	0.48	10.27	2.32
1000	CC	12	1.12	0.56	8.03	4.15
1000	VPC	5	0.78	0.14	4.93	0.69

ness or worse surface quality, respectively. In comparison, the lower filling pressure of the vacuum die cast machine produces significantly lower surface roughnesses. On the other hand, this also causes problems during form filling. Hence the investigator needs to find the optimum for each microstructure balancing the highest necessary filling pressure in order to fill the microcavities against the lowest possible pressure in order to achieve the least surface roughness.

Furthermore, Tables 13-11 and 13-12 show that a higher mold temperature of 1000 °C also has a positive influence on the surface roughness. It is thought that the formation of a thin oxide layer during solidification of the melt causes a smoother surface of the specimens. Therefore, a mold temperature of 1000 °C is beneficial for the form filling and also for a low surface roughness.

13.5.5 Mechanical Properties

In order to understand the relationship between process, microstructure and mechanical properties, tensile tests with microscaled specimens made of a gold base alloy were carried out at the Institute for Materials Science I, University of Karlsruhe, Germany. The specimens have a thickness of 130 µm and a rectangular cross-section with a width of 260 µm. A detailed overview of all results is given in Chapter 19. Here, only the most important results with respect to the casting parameters are presented. This includes the yield stress and the ultimate tensile strength as a function of the mold temperature, the aging condition and the casting procedure (Table 13-13).

For centrifugal casting, an increase in the yield stress and the ultimate tensile stress with increasing mold temperature is observed. A mold temperature of 400 °C, for example, results in a yield stress of 396 MPa. The yield stress increases to 518 and 521 MPa for higher mold temperatures of 700 and 1000 °C, respectively. At the same time, the ultimate tensile stress reaches 628 MPa for a mold temperature of 400 °C and 824 and 776 MPa for the higher mold temperatures. Therefore, in order to achieve a high mechanical strength, for a gold base alloy, a mold temperature between 700 and 1000 °C is required. It has to be

Table 13-13 Mechanical properties of cast Stabilor® G as a function of mold temperature, aging condition and casting procedure[a]

	T_{mold} = 400 °C; CC	T_{mold} = 700 °C; CC	T_{mold} = 1000 °C; CC	T_{mold} = 1000 °C *; CC	T_{mold} = 1000 °C; VPC
Yield stress (MPa)	396	518	521	716	354
Ultimate tensile strength (MPa)	628	824	776	1005	594
No. of specimens	9	8	10	3	9

a CC: centrifugal casting; VPC: vacuum pressure casting; *heat treated (5 h, 800 °C, vacuum).

stressed, however, that these values of mechanical properties are distinctly lower than those given by the manufacturer (measured on macroparts; compare Section 13.3.2). Besides a possible influence of the grain size, this is mostly due to the aging behavior of the cast parts during the cooling phase, because the gold base alloy is a precipitation hardening material which needs to cool slowly. However, for microparts the amount of heat induced by the melt during the casting process is not high enough to generate significant aging while cooling. Therefore, an additional aging process is necessary to achieve full hardening. This can be seen in the fourth column of Table 13-13. The specimens cast in a mold at 1000 °C show an increase in mechanical strength after being heat treated for 5 h at 800 °C in an evacuated quartz tube with subsequent slow cooling inside this set-up. However, the yield strength of the aged microspecimens is distinctly lower than that of their macro specimens while the ultimate tensile stress significantly exceeds the values for macroparts significantly.

Another interesting result is derived from the comparison of the two casting techniques – centrifugal casting and vacuum pressure casting – with respect to the mechanical properties achieved. The centrifugal cast specimens show a yield stress of 521 MPa and an ultimate tensile strength of 776 MPa for a mold temperature of 1000 °C, whereas the vacuum pressure cast specimens show a yield stress of 354 MPa and an ultimate tensile strength of 594 MPa. Here, the much larger grain size of the vacuum cast specimens seems to dominate the results. Investigations reported in Chapter 19 indicate a grain size of 64 µm for these specimens compared with about 10 µm for the centrifugal cast specimens.

13.5.6
Achievable Structure Size, Flow Length and Aspect Ratio

To a great extent, the smallest achievable structure size depends on the aspect ratio, which is defined as the ratio of flow length to wall thickness. Investigations showed that very small structures can be cast with the gold base alloy owing to its good flowability and form filling behavior. Wall structures down to 20 µm width were produced with an aspect ratio of 6. If adequate patterns were available, even smaller structures should be castable with this alloy. The smallest structures cast with all three alloys in this project, the gold base alloy Stabilor® G, the Al-bronze and the CoCrMo alloy Biosil® f, are channels on a turbine plate with a width of 25 µm and a structure height of 350 µm.

The flow length and aspect ratio achievable are mainly influenced by the preheating temperature of the ceramic mold and by the filling pressure. Flow length tests were carried out in order to determine the dependence of these two parameters on the form filling behavior. Therefore, two different fiber patterns were produced which consist of 10 organic fibers each mounted on a horizontal wax sprue. In the first case the fibers had a diameter of 210–230 µm and in the other case the diameter was 100 µm. The fibers were cast in the gold base alloy Stabilor® G and in Al-bronze using different mold temperatures and filling pressures. The results of the flow length tests are presented in Fig. 13-19. For

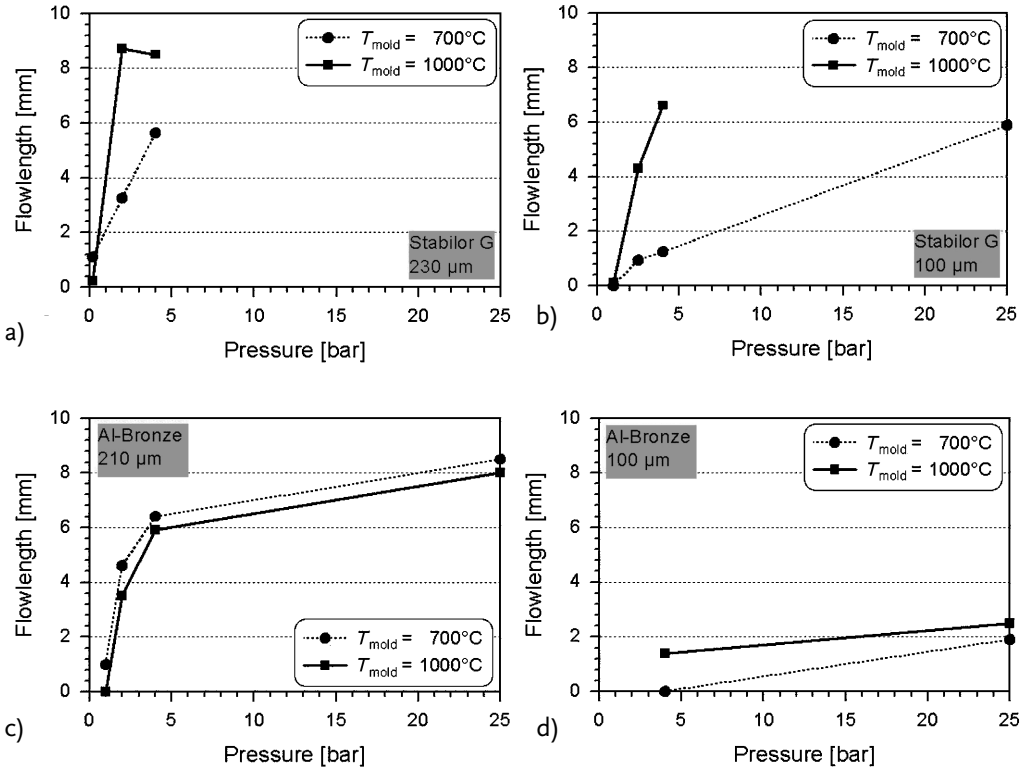

Fig. 13-19 Flow lengths of different metal melts during form filling of Stabilor® G in holes with different diameters in the submillimeter range. a) Stabilor® G (230 µm); b) Stabilor® G (100 µm), c) Al-bronze (210 µm), d) Al-bronze (100 µm)

Stabilor® G, with a fiber diameter of 230 µm (Fig. 13-19a) and a mold temperature of 1000 °C, which exceeds the liquidus temperature of 940 °C, the maximum flow length of about 9 mm is reached at a relatively low pressure of 2 bar. For a mold temperature of 700 °C, a linear increase in flow length with increasing pressure is observed. Here, a pressure of 4 bar – the value where the vacuum pressure casting machine is at its limit – results in a flow length of nearly 6 mm. For a fiber diameter of 100 µm (Fig. 13-19b), the same value can be reached at a pressure of 25 bar using the centrifugal casting machine. In summary, for a mold temperature of 700 °C an increase in pressure from 4 to 25 bar allows the fiber diameter to be halved while achieving the same flow length. This corresponds to an aspect ratio of 60.

For the Al-bronze, there is a more pronounced difference in achievable flow lengths dependending on the fiber geometry. Whereas for fibers with a diameter of 210 µm (Fig. 13-19c) the flow length increases similarly for the two mold temperatures with increasing pressure, for fibers with a diameter of 100 µm

(Fig. 13-19 d) a flow length of only about 2 mm was reached, resulting in an aspect ratio of 20. Hence the improvement regarding the flow length achievable by increasing the pressure is very small. The reason for this behavior is the distinctly higher solidification temperature of Al-bronze compared with the gold base alloy Stabilor® G. Consequently, the much larger difference between mold and solidification temperature for the Al-bronze yields a much faster solidification of the bronze melt when entering the mold compared with the melt of the gold base alloy and, therefore, an increase in pressure has only a small influence on the achievable flow length of the Al-bronze.

In addition, the different solidifications of the two alloys, Al-bronze and Stabilor® G, should be taken into account. Whereas the gold base alloy is a solid solution with very fine precipitations, the Al-bronze forms a much coarser multiphased microstructure which is likely to be detrimental to the form filling of extremely fine structures. It is therefore suggested that, compared with Stabilor® G, the use of Al-bronze should be limited to microstructures with lower aspect ratios than for Stabilor® G. However, these limitations might only cause problems for extremely fine structures with aspect ratios of >20 and diameters <100 µm. Current research has shown that all microstructures mentioned in this chapter can be cast with Al-bronze. Even the tensile test specimens with an aspect ratio of 30 and a wall thickness of only 130 µm were castable with this material, because their cross-sectional area (33 800 μm^2) is comparable to that of fibers with a diameter of 210 µm (34 636 μm^2).

Therefore, microcasting is an ideal processing tool for the replication of nearly all microstructures with large flow lengths or large aspect ratios, even if the wall thicknesses reach a minimum value.

13.6 Conclusions

Investment casting is a suitable technique for the manufacture of metallic microparts. The smallest channel structures cast with all three alloys tested, a gold base alloy (Stabilor® G), an Al-bronze alloy and a CoCrMo alloy, have a width of 25 µm and a height of 350 µm. In addition, with Stabilor® G even smaller wall structures 20 µm wide and 120 µm high could be cast. Nevertheless, the dimensional limits for microcasting have not been reached yet. Especially gold base alloys such as Stabilor® G offer the potential for further miniaturization of investment cast components.

The results of microcasting depend on several parameters such as filling pressure and mold temperature which are of special importance. It has been shown that with our equipment centrifugal casting provides a significantly higher filling pressure than vacuum pressure casting. Thus centrifugal casting is of advantage when long and thin fiber-like parts are to be cast. The mold temperature has a significant influence on the average grain size of cast specimens. The grain size of vacuum pressure cast specimens with a diameter of 3 mm

and a length of about 25 mm increases for the gold alloy from about 24 μm to 91 μm and for the Al bronze from 30 μm to 170 μm when the mold temperature is increased from 100 °C to 1000 °C.

The casting result is also influenced by the surface structure, i.e. the porosity of the mold. A modification of a commercial, phosphate-bonded investment reduces the surface roughness from $R_a = 1.13$ μm to $R_a = 0.44$ μm compared to the commercial investment. Furthermore, the dimensional accuracy of the cast parts is determined by the expansion behavior of the investment which needs to be in compliance with the shrinking of the cast metal during solidification and cooling. Here, for bending bars with a nominal width of 200 μm, a deviation of only 1.5 μm between cast parts and patterns was achieved.

The achievable flow lengths are determined by the casting material, the filling pressure and the mold temperature. An aspect ratio of 60 was reached for the gold base alloy Stabilor® G and a filling pressure of about 25 bar, even for a relatively low mold temperature of 700 °C. But Al-bronze also allows for aspect ratios which are sufficient for most applications within the collaborative research center.

In summary, the investigations have demonstrated that microcasting is an ideal fabrication method for metal parts in microdimensions, e.g. for a demonstrator consisting of a gear unit and a turbine, in small and medium series production. A further advantage of microinvestment casting, i.e. the possibility of casting real three-dimensional microstructures even with undercuts, will be explored in the near future. In addition, for a higher level of automation, the development of a microchill-mold technique using permanent molds instead of lost molds may be promising.

13.7 References

1 Fr.-W. Bach, K. Moehwald, U. Hollaender, B. Nakhosteen, *Z. Metallkd.* **2001**, 92, 207–211.

2 K. Moehwald, C. Morsbach, Fr.-W. Bach, H.-H. Gatzen, in: *1st International Conference and General Meeting of the European Society for Precision Engineering and Nanotechnology*, Bremen: Shaker Verlag, **1999**, Vol. 1, pp. 490–493.

3 H. Wöllmer, *Nachr. Forschungszentrum Karlsruhe*, **1998**, *30*, 237–242.

4 H. Woellmer, K. Mueller, R. Ruprecht, J. Hausselt, presented at the European Conference Junior EUROMAT'98: Conf. on Materials and Nuclear Power, Lausanne, 11–17 September **1998**.

5 H. H. Caesar, *Dent. Labor* **1988**, 36 (2), 189–201.

6 H. H. Caesar, *Dent. Labor* **1988**, 36 (3), 317–322, 325, 328.

7 R. F. Smart, Investment Casting; Foundry Trade Journal, **1990**, 164; 2–4.

8 Degussa Dental GmbH AG, *Edelmetall-Taschenbuch*; Hüthig, Heidelberg, **1995**.

9 J. Hausselt, in *Enzyklopädie der Naturwissenschaft und Technik*; Munich: Verlag Moderne Industrie, **1979**, 807–810.

10 J. Hausselt, in *Enzyklopädie der Naturwissenschaft und Technik*, Munich: Verlag Moderne Industrie, **1979**, 957–964.

11 J. Hausselt, W. Kempf, *Interdiscip. Sci. Rev.* **1992**, *17*, 251–260.

12 E. Drost, J. Hausselt, *Interdiscip. Sci. Rev.* **1992**, *17*, 271–280.

13 B. Kempf, „Dentalwerkstoffe“ in: *Enzyklopädie Naturwissenschaft und Technik*, 2. Auflage, Ecomed-Verlag, **1996**, D7–10.
14 K. Eichner, *Zahnärztliche Werkstoffe und ihre Verarbeitung*; Heidelberg: Hüthig Verlag, **1996**.
15 G. Baumeister, R. Ruprecht, J. Hausselt, *Microsyst. Technol.* **2004**, *10*, 484–488.
17 S. Rath, G. Baumeister, J. Hausselt, *Microsyst. Technol.*, to be published.
18 Ch. Corti, *Gold Technol.* **2000**, (28), 27–32.
19 T. Schaller, M. Heckele, R. Ruprecht, presented at the ASPE 1999 Spring Topical Meeting, Chapel Hill, NC, USA, June **1999**.
20 J. Schmidt, H. Tritschler, H. Haberer, in: *Proc. of the 2nd Int. Conf. of the EUSPEN, 30 May 2001, Turin*; **2001**, 624–627.
21 H. Weule, V. Hüntrup, H. Tritschler, *Ann. CIRP* **2001**, *50*, 61–64.
22 J. Schmidt, M. Simon, H. Tritschler, R. Ebner, *wt Werkstattstechnik online* **2001**, *91*, H.12., 743–746.
23 J. Fleischer, T. Masuzawa, J. Schmidt, M. Knoll, *J. Mater. Process. Technol.* **2004**, *149*, 246–249.
24 W. Pfleging, T. Hanemann, M. Torge, W. Bernauer, *Proc. Inst. Mech. Eng. C, J. Mech. Eng. Sci.* **2003**, *217*, 53–63.
25 W. Pfleging, W. Bernauer, T. Hanemann, M. Torge, *Microsyst. Technol.* **2002**, *9*, 67–74.
26 W. Jiang, P. Molian, *Int. J. Adv. Manuf. Technol.* **2002**, *19*, 646–654.
27 W. Bacher, K. Bade, B. Matthis, M. Saumer, R. Schwarz, *Microsyst. Technol.* **1998**, *4*, 117–119.
28 A. Rogner, J. Eicher, D. Muenchmeyer, R.-P. Peters, J. Mohr, *J. Micromech. Microeng.* **1992**, *2*, 133–140.
29 W. Ehrfeld, V. Hessel, H. Loewe, Ch. Schulz, L. Weber, *Microsyst. Technol.* **1999**, *5*, 105–112.
30 J. Hruby, *MRS Bull.* **2001**, April, 1–4.
31 G. Baumeister, K. Mueller, R. Ruprecht, J. Hausselt, *Microsyst. Technol.* **2002**, *8*, 105–108.
32 M.A. Gwyn, *Engineered Casting Solutions* **2002**, Summer, 2002, 66, or see technical articles in *http://www.castingsource.com*
33 S. Guleyupoglu, *Casting Process – Design Guidelines, http://www.moderncasting.com/archive/transactions/97-083.pdf* March **2000**; or *The Basics of Feeding Steel and Ductile Iron Castings, http://www.moderncasting.com/archive/feature_040.asp* March **2000**.
34 M.T. Manzari, R.aW. Lewis, D. Gethin, J.T. Cross, in: *Proceeding of OptiCON*; *swan.ac.uk*.
35 R. Kotschi, in: *Metals Handbook, Vol. 15, Casting*, 9th edn.; Metals Park OH: ASM International, **1988**, pp. 598–613.
36 W. Schal, *Fertigungstechnik 2*; Hamburg: Verlag Technik und Handwerk, **1992**, Ch. 2.1.5.
37 E. Bell, *Gold Technol.* **2002**, (36), 3–11.
38 R. Horton, in: *Metals Handbook, Vol. 15, Casting*, 9th edn.; Metals Park OH: ASM International, **1988**, 251–269.
39 D. Ott, *Handbook on Casting and Other Defects*; London: World Gold Council, **1997**.
40 V. Faccenda, *Handbook on Investment Casting*; London: World Gold Council, Ch. 2, **2003**, 56–57.
41 D. Ott, Analysis of common casting defects, *Gold Technol.* **1994**, (13), 2–15.
42 D. Ott, *Gold Technol.* **1994**, (13), 16–22.
43 M.F. Grimwade, *Gold Technol.* **1990**, (2), 11–16.
44 M. Grimwade, *Gold Technol.* **2000**, (29), 2–15.
45 G. Baumeister, K. Mueller, R. Ruprecht, J. Hausselt, *Microsyst. Technol.* **2002**, *8*, 105–108.
46 *Manual Ticast Super R*; Osaka: Kobelco Research Institute.
47 *http://www.degudent.de/Produkte/Geraete/Multicast_compact.asp*
48 *http://www.degudent.de/Produkte/Geraete/Motorcast_compact.asp*
49 *http://www.bego.com/html/e/p/product8.shtml*
50 *http://www.selec-inc.com/eng/eng_castmachine01.html*
51 V. Faccenda, *Gold Technol.* **1998**, (23), 21–26.
52 *Deguvest® CF, HFG and F, Instructions for Use*; Hanau: Degussa Dental GmbH.
53 Sir L. Woolley, *Ur-Excavations*; London, 1934, Vol. II, 78.
54 L.B. Hunt, *Gold Bull.* **1980**, *13*, 63–79.
55 Ch. Raub, *Metall* **1981**, *35*, 1257–1259.
56 T.G.H. James, *Gold Bull.* **1972**, *5*, 38–42.

57 B. Kempf, J. Hausselt, *Interdiscip. Sci. Rev.* **1992**, *17*, 251–260.

58 K. F. Leinfelder, D. F. Taylor, *J. Dent. Res.* **1977**, *56*, 335–345.

59 K. Yasuda, M. Ohta, *J. Dent. Res.* **1982**, *61*, 473–479.

60 K.-I. Udoh, H. Fujiyama, K. Hisatsune, M. Hasaka, K. Yasuda, *J. Mater. Sci.* **1992**, *27*, 504.

61 H. I. Kim, M. I. Jang, B. J. Jeon, *J. Mater. Sci. Med.* **1997**, *8*, 333–339.

62 K. Hamasaki, K. Hisatsune, K. Udoh, Y. Tanaka, Y. Iijima, O. Takagi, *J. Mater. Sci. Med.* **1998**, *9*, 213–219.

63 K. Yasuda, *Gold Bull.* **1987**, *20*, 90–103.

64 Y. Li, T. G. Ngai, *J. Mater. Sci.* **1996**, *31*, 533–538.

65 R. J. C. Dawson, *Eng. Mater. Des.* **1978**, *22*, 25.

66 G. Benkisser, I. Ruehl, C. Ladewig, *Prakt. Metallogr.* **2001**, *38*, 425–441.

67 G. Horn-Samodelkin, G. Winkel, I. Ruehl, *Metall* **1996**, *50*, 44–49.

68 R. Kainuma, S. Takahashi, K. Ishida, *Met. Mater. Trans. A* **1996**, *27*, 2187–2195.

69 H. B. Skinner, in: *Current Diagnosis and Treatment in Orthopedics*; Norwalk, CT: Appleton and Lange, **1995**, 19.

70 D. F. Williams, in: *Materials Science and Technology, Vol. 14, Medical and Dental Materials*, R. W. Cahn, P. Hansen, E. J. Kramer (eds.); Weinheim: Wiley-VCH, **1992**, Ch. 1.

71 D. H. Kohn, P. Ducheyne, in: *Materials Science and Technology, Vol. 14, Medical and Dental Materials*, R. W. Cahn, P. Hansen, E. J. Kramer (eds.); Weinheim: Wiley-VCH, **1992**, Ch. 2.

72 A. Kulmburg, G. Kvas, G. Wiedner, P. Golob, P. Warbichler, M. Schmied, R. O. Bratschko, *Prakt. Metallogr.* **2001**, *38*, 514–531.

73 A. J. T. Clemow, B. L. Daniell, *J. Biomed. Mater. Res.* **1979**, *13*, 265–279.

74 T. Kilner, R. M. Pillar, G. C. Weatherly, C. Allibert, *J. Biomed. Mater. Res.*, **1982**, *16*, 63–79.

75 C. P. Sullivan, M. J. Donachie Jr., F. R. Morral, *Cobalt Superalloys*; Brussels: Centre d'Information de Cobalt, **1979**.

76 *Biosil®, Instructions for Use*; Hanau: Degussa Dental GmbH.

77 H. H. Schulz, *Dental-Labor* **1976**, *24*, 339–344.

78 H. Salmang, H. Scholze, *Keramik*; Berlin: Springer, **1986**.

79 Degussa Dental GmbH, Hanau, personal communications and information.

80 H.-W. Gundlach, in *Zahnärztliche Werkstoffe und ihre Verarbeitung*, K. Eichner, H. F. Kappert (eds.); Heidelberg: Hüthig Verlag, , **1996**, Vol. 1, Ch. 2.

81 D. Low, M. V. Swain, *J. Mater. Sci.: Mater. Med.* **2000**, *11*, 399–405.

82 L. Borchers, in: *Zahnärztliche Werkstoffe und ihre Verarbeitung*, K. Eichner, H. F. Kappert (eds.); Heidelberg: Hüthig Verlag, **1996**, Vol. 1, Ch. 1.

83 R. Carter, *Gold Technol.* **2001**, (32), 7–18

84 G. Baumeister, S. Rath, R. Ruprecht, J. Hausselt, *Proc. Mater. Week*, **2001**, Munich (CD-ROM)

85 *http://www.sfb499.de/*

86 *ASME/ANSI B46.1, Surface Texture (Surface Roughness, Waviness and Lay)*, New York: American Society of Mechanical Engineers (ASME), **1995**.

87 *DIN EN ISO 4287. Geometrische Produktspezifikationen (GPS) – Oberflächenbeschaffenheit: Tastschnittverfahren – Benennung, Definition und Kenngrößen der Oberflächenbeschaffenheit*; Release 1998-10.

88 *DIN 4768*; **1990-05**. *Ermittlung der Rauheitskenngrößen R_a, R_z, R_{max} mit elektrischen Tastschnittgeräten – Begriffe, Meßbedingungen*; Release

89 R. Papst, *Ermittlung von mechanischen Kennwerten an Mikrozugproben aus Stabilor G® (Au58Ag23Cu12) unter Zuhilfenahme des Verfahrens der optischen Dehnungsmessung*, Report of the Institute for Materials Research I, University of Karlsruhe (TH), Germany, Karlsruhe: Karlsruhe University, **2004**, Ch. 5.1.2.